Article:
Everett, Gabriella, Hodnebrog, Øivind, Agrawal, Madhoolika et al. (2025) Ozone pollution may limit the benefits of irrigation to wheat productivity in India. Biogeosciences. pp. 4203-4219. ISSN: 1726-4189

https://doi.org/10.5194/bg-22-4203-2025

Biogeosciences, 22, 4203–4219, 2025
https://doi.org/10.5194/bg-22-4203-2025

Biogeosciences Open Access EGU

Ozone pollution may limit the benefits of irrigation to wheat productivity in India

Gabriella Everett[1], Øivind Hodnebrog[2], Madhoolika Agrawal[3], Durgesh Singh Yadav[4], Connie O'Neill[5], Chubamenla Jamir[6], Jo Cook[1,5], Pritha Pande[1], Sam Bland[5], and Lisa Emberson[1]

[1]Department of Environment and Geography, University of York, York, YO10 5DD, UK
[2]CICERO Center for International Climate Research – Oslo, 0318, Oslo, Norway
[3]Department of Botany, Institute of Science, Banaras Hindu University, Varanasi 221005, India
[4]Department of Botany, Government Raza P.G. College, Rampur, U.P. 244901, India
[5]Stockholm Environment Institute, University of York, York, YO10 5DD, UK
[6]Climate Studies and Knowledge Solutions Centre, Kohima, Nagaland, India

Correspondence: Lisa Emberson (l.emberson@york.ac.uk)

Received: 31 October 2024 – Discussion started: 15 November 2024
Revised: 8 May 2025 – Accepted: 11 May 2025 – Published: 26 August 2025

Abstract. Ground-level ozone (O_3) pollution and heat and water stress are recognised as key abiotic stresses which threaten the ability of wheat yields to meet the growing demand for food production in India. The magnitude and interplay of O_3 and water stress effects are tightly coupled via stomatal conductance and the transpiration pathway. Existing modelling methods that assess the stress response as a function of O_3 and water vapour stomatal flux are applied to assess O_3's role in limiting the productivity afforded by irrigation. We investigate the effect of these stresses on the grain yield of older (HUW-234) vs. recently released (HD-3118) Indian wheat cultivars under recent-past and future climates and O_3 precursor emission profiles (using RCP4.5 and RCP8.5 scenarios). Water stress in rainfed conditions was modelled to analyse the trade-off between O_3-induced vs. water-stress-induced yield loss to quantify the extent to which water stress mitigates O_3 stress via reduced stomatal conductance. Under rainfed conditions for the years 1996–2005, the mean water-stress-induced and O_3-induced yield losses for HUW-234 were 13.3 % and 0.6 %, respectively. The latter was a significant decrease from the mean O_3-induced yield loss of 10.6 % modelled under irrigated conditions (i.e. no water stress). Similarly, under the RCP4.5 and RCP8.5 scenarios for the mid-century, water-stress-induced yield losses under rainfed conditions were 10.1 % and 20.0 %, while mean O_3-induced yield losses were only 1.0 % and 0.1 %, respectively. Under irrigation, O_3-induced yield losses increased to 18.5 % and 13.7 %, suggesting that O_3 stress will negate the beneficial effects of irrigation. The cultivar HD-3118 suffered, on average, 0.2 % greater O_3 relative yield loss (O_3-RYL) than HUW-234 across all scenarios. The O_3-RYL increased with climate change by 7.9 % under the RCP4.5 scenario and by 3.0 % under the RCP8.5 scenario compared to the recent-past climate. Together, these findings suggest that O_3 may continue to substantially limit the productivity benefits of the use of modern cultivars bred for high gas exchange under irrigated conditions in India.

1 Introduction

Wheat is a vital crop for India's economy and food security; India is the second largest wheat producer in the world, and most of its population gains > 50 % of their calorific intake from this staple grain (Tripathi and Mishra, 2017). With India's population of 1.4 billion growing at a rate of 2.23 % yr^{-1} (UNDESA, 2022), wheat will play a major role in ensuring that food supply meets the growing demand (Tripathi and Mishra, 2017). However, India's croplands are exposed to particularly high O_3 concentrations ($[O_3]$), with hotspots occurring across the Indo-Gangetic Plains (IGP) (Roy et al., 2008). The 8 h daily mean O_3 concentrations often reach up to 100 ppb in hotspots during the Rabi crop-growing season (October to April) and are therefore a sig-

nificant threat to India's wheat productivity (Deb Roy et al., 2009). Currently, there are no air quality standards in India to protect crops from surface O_3, and emissions of O_3 precursors are forecast to continue to rise well into the 21st century, driven by persistent growth in industries, including mining and petroleum industries; vehicular traffic; and agricultural activities (Ghude et al., 2014; Sharma et al., 2019; Yadav et al., 2019). Ozone distribution varies spatially and temporally, but the IGP region often experiences high levels due to the long-distance transport of O_3 and its precursors from urban, industrial, or power generation centres located across northern India (Singh and Agrawal, 2017).

Ozone damages crops when it diffuses into the intracellular airspace of the leaf via the stomata, which triggers a cascade of metabolic and physiological responses resulting in reduced carbon assimilation, premature leaf senescence, and visible injury. Together, these effects can lead to reductions in the overall yield and quality (Emberson et al., 2018). Since O_3 damage relies on stomatal O_3 flux (i.e. O_3 dose), the scale of damage caused by ambient [O_3] varies with stomatal conductance. Stomatal conductance is determined, in the short term, by environmental factors that trigger the closure of the stomata and, in the long term, by adaptations to climate change, i.e. reduced stomatal density (Emberson et al., 2018). Two other factors also influence a crop's vulnerability to O_3 dose, namely its detoxification ability and the signal transduction pathway, which regulates the response of cells to the increased oxidative load caused by O_3 (Ainsworth et al., 2008; Kangasjärvi et al., 2005).

It is widely acknowledged that stress conditions including elevated levels of carbon dioxide (CO_2), heat, water vapour pressure deficit (VPD), and soil water deficit (all of which may be associated with climate change) decrease stomatal conductance, thus reducing O_3 flux in wheat and potentially ameliorating O_3 damage to the photosynthetic apparatus (Feng et al., 2008). In addition, several studies have found that modern cultivars are more O_3 sensitive due to selection for enhanced gas exchange, which could counteract their natural adaptation of lower stomatal conductance in response to the changing climate. Pleijel et al. (2006) and Yadav et al. (2020) observed greater O_3-related yield loss in a modern wheat cultivar, HD-3118, bred for a higher yield than HUW-234, which was attributed to the cultivar's higher stomatal density and conductance. Climate change is expected to increase the use of drought-resistant cultivars which can maintain higher stomatal conductance under drought conditions; this will likely increase crop sensitivity to O_3 (Emberson et al., 2018). Eliminating the use of cultivars with higher stomatal conductance is unlikely to improve productivity because, on a broader scale, yield losses due to water stress outweigh those from O_3 (Emberson et al., 2018). However, in major wheat-producing states like Uttar Pradesh, where irrigation is widespread (Zaveri and Lobell, 2019), yield losses due to O_3 may outweigh those due to water stress; hence, the use of cultivars with a lower stomatal conductance may be beneficial.

Khan and Soja (2003) found that well-irrigated wheat plants (i.e. with a 75 % soil water capacity (SWC)) suffered grain yield losses of up to 39 % when exposed to accumulated O_3 concentrations over a threshold of 40 ppb (AOT40) of $\sim 25\,\mathrm{ppm\,h^{-1}}$. Under severe moisture deficits (35 % SWC), no O_3-related yield loss was observed as O_3 uptake was reduced by up to 90 %. However, the grain yield of water-stressed wheat was significantly less than that of well-watered wheat. In a similar study by Harmens et al. (2019) on wheat in Africa, grain yield loss due to O_3 exposure was greater in well-watered plants than in crops that received reduced irrigation, suggesting controlled irrigation as a management tool to reduce O_3 impact. Whilst drought reduces yields at all stages of development, drought stress during anthesis and grain filling causes the greatest yield reductions (Farooq et al., 2014). Additionally, anthesis and grain filling are when wheat is most sensitive to [O_3] and constitute the period of time when the [O_3] concentrations are highest during the Indian growing season (Gelang et al., 2000; Pleijel et al., 1998; Rathore et al., 2023). Several experimental studies have investigated the interaction between O_3 and drought stress in wheat. While some studies have observed no significant interactions between increased [O_3] and water stress (Broberg et al., 2023; Fangmeier et al., 1994), others have observed an interaction. Ghosh et al. (2020) observed an additive effect of O_3 and drought stress, with a greater reduction in grain yield when both stressors occurred simultaneously due to the reduction in nutrient uptake and assimilation. As a result of these contrasting findings, it is evident that the trade-offs between O_3 exposure and water stress require further study.

Irrigation has the potential to maximise O_3 stress by providing conditions that are likely to enhance stomatal conductance, such as plentiful soil and leaf water, transpirational cooling, and a low leaf-to-air VPD. Irrigation is widespread across the IGP, particularly in the states of Punjab, Haryana, and Uttar Pradesh; the areas irrigated as a percentage of the total area of wheat were 99.1 %, 99.9 %, and 99 %, respectively, in 2018–2019 (Ministry of Agriculture & Farmers Welfare, 2022), which means that current wheat crop management practices are likely to enhance sensitivity to O_3. Modifying irrigation practices has been suggested as a strategy to reduce O_3 damage, but caution is needed to avoid introducing water stress, which could also negatively affect yield (Harmens et al., 2019; Teixeira et al., 2011). Irrigation has additional benefits and has often been implemented to offset heat-related yield losses which occur when temperatures exceed 35 °C (Zaveri and Lobell, 2019). However, studies suggest that sustainable use of India's future groundwater availability with current irrigation practices would mitigate less than 10 % of the climate change impact on crop yield (Fishman, 2018). Additionally, water for irrigation purposes is limited; for example, Zaveri et al. (2016) found that Uttar

Pradesh will lack scope for further increasing irrigation as groundwater depletion escalates due to climate change and increasingly unsustainable water demand. With irrigation accounting for up to 90 % of India's total water demand, water efficiency in agriculture is a priority in the IGP to achieve better environmental and economic performance (Fischer et al., 2007; Wada et al., 2013). Here, we explore the interplay between O_3- and water-stressed-induced yield losses, which will help inform us on whether or not water efficiencies could also provide some benefits in terms of the decreased sensitivity of staple crops to O_3.

There have been an increasing number of studies exploring the effect of O_3 on wheat yields using a cumulative stomatal O_3 flux metric (POD_Y; phytotoxic O_3 dose over a flux threshold Y), which accounts for the stomatal response to environmental conditions and plant growth stages that alter O_3 uptake. By comparison, concentration-based exposure metrics such as AOT40 only account for atmospheric [O_3], which may be decoupled from O_3 uptake under environmental conditions that limit stomatal conductance; they also omit O_3 concentrations below 40 ppb, which are known to be capable of causing damage (CLRTAP, 2017; Emberson et al., 2018). Mills et al. (2018a) estimated an O_3-induced yield loss that incorporated the effects of irrigation to be in the range of 15 %–20 % for wheat growing in Uttar Pradesh between 2010–2012 using POD_3IAM (POD above 3 nmol m^{-2} s^{-1}, parameterised for integrated assessment modelling) (CLRTAP, 2017). This parameterisation was based on European wheat cultivars and a broad-scale assessment of India's wheat-growing season, with the POD_3IAM metric being applied according to the formulations of the Deposition of Ozone for Stomatal Exchange (DO_3SE) model (Büker et al., 2012; CLRTAP, 2017; Emberson et al., 2000a, 2018). An alternative metric used in estimations of stomatal O_3 flux effects on crops is POD6SPEC, which is the species-specific phytotoxic O_3 dose above 6 nmol m^{-2} s^{-1}. This metric is better suited for local to regional risk assessments (CLRTAP, 2017).

Application of the stomatal O_3 flux method allows for an exploration of the relative effects of both O_3 and water stress on yield since the DO_3SE model also estimates water vapour fluxes based on which potential and actual evapotranspiration can be calculated (Büker et al., 2012). In this study, we parameterise the DO_3SE model (version 3.1.0; Bland et al., 2025) for two late-sown Indian wheat cultivars for the estimation of the POD_6SPEC metric. We apply the Weather Research and Forecasting model with Chemistry (WRF-Chem) (Grell et al., 2005) to obtain [O_3] and climate variable data for Varanasi, Uttar Pradesh. We compare O_3 effect yield losses (using the wheat grain yield flux–effect relationship (CLRTAP, 2017)) with yield losses due to water stress based on yield responses to the ratio of actual vs. potential evapotranspiration (see Steduto et al., 2012). This modelling setup allows us to explore the relative magnitude of yield losses from O_3 and water stress, how these are likely to change in the future, and the relative sensitivities of older vs. more recently released Indian cultivars to damage from O_3 pollution.

2 Methods

For this study, Varanasi was selected as the study area due to (i) its location in the important wheat-growing IGP and (ii) the availability of observed crop and O_3 data.

2.1 Experimental data

Experimental data from the period of 2016–2018 were obtained for two late-sown Indian spring wheat (*Triticum aestivum* L.) cultivars grown at the Botanical Garden of Banaras Hindu University (BHU), Varanasi (25°16′ N, 82°59′ E; 81.0 m above sea level). HUW-234 (released in 1986 by BHU, Varanasi) and HD-3118 (released in 2014 by IARI, New Delhi) were selected based on their heat tolerance and extensive cultivation in the North East Plain Zone of India (Joshi et al., 2007; Yadav et al., 2019). The recently released cultivar, HD-3118, is more highly yielding (6.64 t ha^{-1}) compared to HUW-234 (4.5–5 t ha^{-1}), most likely due to its enhanced capacity for gas exchange. This enhanced capacity for gas exchange is the likely reason for the HD-3118 cultivar having a greater sensitivity to O_3 than the HUW-234 cultivar (Yadav et al., 2020).

2.2 Modelled data

Hourly meteorological and O_3 data for the Varanasi grid box (45 km × 45 km horizontal resolution) were obtained by running WRF-Chem v.3.8.1 for the years 1996–2005 (considered to be the "recent-past" climate) and 2046–2055 using both RCP4.5 and RCP8.5 climate scenarios. The 45 km resolution model domain is the same as in Daloz et al. (2021), and the meteorological initial and boundary conditions come from global climate model simulations with the Community Earth System Model (CESM) v.1.0.4 (Gent et al., 2011), as documented in Hodnebrog et al. (2019). The WRF-Chem simulations are set up with the RADM2 gas-phase chemistry scheme (Stockwell et al., 1990), and O_3 precursor emissions are from Lamarque et al. (2010) for the historical period and from Lamarque et al. (2011) for the future RCPs (Representative Concentration Pathways). Global mean CO_2 mixing ratios (ppm) for 1996–2005 were obtained from NASA (using Tans and Conway (2020) for 1983–2003 and Conway (2020) for 2004–2007). For future scenarios, RCP4.5 and RCP8.5 [CO_2] values for 2046–2055 were acquired (Meinshausen et al., 2011). WRF-Chem with the RADM2 chemical mechanism has been found to reproduce diurnal average O_3 over India in February–May relatively well, while noontime O_3 concentrations show considerable differences between simulations with various emission inventories (Sharma et al., 2017).

The RCP climate scenarios are selected to provide a range of climate and pollution futures for India from which a consequent range in yield responses can be estimated. RCPs are possible greenhouse gas (GHG) emission pathways designed to aid research into climate change impacts (Riahi et al., 2011). RCP8.5 is a very high baseline, representing the highest GHG emission pathway in a "business-as-usual" scenario, resulting in a radiative forcing of 8.5 W m^{-2} at the close of the 21st century, equivalent to 1370 ppm [CO_2] (He and Zhou, 2015; Riahi et al., 2011). RCP4.5 is a medium-stabilisation scenario where global climate policy values the role of natural carbon sequestration and land use, resulting in a radiative forcing target of 4.5 W m^{-2} (650 ppm [CO_2] equivalent) for 2100 (Riahi et al., 2011; van Vuuren et al., 2011).

These data provided inputs for the DO_3SE model, which was used to simulate stomatal O_3 flux values and water stress characteristics for the two cultivars for each year. For the modelled climate, O_3 and CO_2 data for the recent-past climate and both RCP scenarios are summarised in Table 1. The modelled temperature data are, on average, 1.3 °C warmer in the RCP4.5 scenario and 1.9 °C warmer in the RCP8.5 scenario than the recent-past modelled climate.

2.3 Model formulation – O_3-induced yield loss estimates

The DO_3SE model (version 3.1.0; Bland et al., 2025) (https://www.sei.org/projects-and-tools/tools/do3se-deposition-ozone-stomatal-exchange/, last access: 22 July 2025) was used to estimate stomatal O_3 flux and subsequent O_3-induced yield loss for wheat. DO_3SE is a dry-deposition model which takes into account the influence of climatic, soil, and plant factors on stomatal conductance to estimate stomatal O_3 flux and to determine the accumulated stomatal O_3 uptake during a specified growth period: POD_Y (CLRTAP, 2017). The stomatal-conductance (g_{sto}) multiplicative algorithm – see Eq. (1) – used in DO_3SE estimates hourly g_{sto} to O_3 by modifying a species-specific maximum g_{sto} (g_{max}) according to environmental variables and is described in Emberson et al. (2000a, b).

$$g_{sto} = g_{max} \times \left[\min\left(f_{phen}, f_{O_3}\right)\right] f_{light} \times \\ \times \max\left\{f_{min}, \left(f_{temp} \times f_{VPD} \times f_{sw}\right)\right\} \quad (1)$$

In the above, g_{sto} and g_{max} are expressed in mmol O_3 m^{-2} PLA s^{-1}. The factors f_{phen}, f_{O_3}, f_{light}, f_{temp}, f_{VPD}, f_{sw}, and f_{min} represent the influence of phenology, [O_3], light, air temperature, VPD, soil water potential, and minimum g_{sto} and are expressed in relative terms as a proportion of g_{max} (and so have a value between 0–1). Functions describing these factors for environmental conditions are described in CLRTAP (2017) based on European wheat varieties; for f_{sw} (and to simulate g_{sto} for rainfed wheat), we assume a linear relationship between a relative g_{sto} of 1 and f_{min} at soil water potentials (SW) of −0.3 and −1.1 MPa (Ali et al., 1999; Morgan, 1984). To simulate the g_{sto} of irrigated wheat, we simply assume that f_{sw} is always equal to 1.

Stomatal O_3 flux (F_{st}; nmol m^{-2} PLA s^{-1}) was calculated using Eq. (2).

$$F_{st} = c\,(z_i) \times g_{sto} \times \frac{r_c}{(r_b + r_c)} \quad (2)$$

In the above, $c\,(z_i)$ is [O_3] at the top of the canopy height i (m), and r_c and r_b represent leaf surface and quasi-laminar leaf boundary layer resistances, respectively, based on leaf dimension and wind speed (CLRTAP, 2017).

The species-specific POD_Y (POD_YSPEC) is estimated for the wheat accumulation period according to Eq. (3).

$$POD_Y SPEC = \sum\left[(F_{st} - Y) \times \left(\frac{3600}{10^6}\right)\right] \quad (3)$$

In the above, Y (nmol O_3 m^{-2} PLA s^{-1}) is subtracted from F_{st} (in nmol m^{-2} PLA s^{-1}) when $F_{st} > Y$ during daylight hours; this Y value represents the assumed detoxification capacity of wheat in relation to O_3 flux. The value is then converted into hourly fluxes by multiplying by 3600 and into mmol by dividing by 10^6 to give POD_YSPEC in mmol O_3 m^{-2} PLA (CLRTAP, 2017). A Y value of 6 nmol m^{-2} PLA s^{-1} was used based on values for European wheat (CLRTAP, 2017). The resulting POD_6SPEC values were used to estimate the percentage grain yield (relative to 100 % grain yield under pre-industrial O_3 conditions) based on the dose–response relationship in Eq. (4).

$$\%\ \text{grain yield} = 100.3 - (3.85 \times POD_6 SPEC) \quad (4)$$

The relationship in Eq. (4) is taken from CLRTAP (2017), where relative grain yields from five wheat cultivars in four European countries were regressed against the POD_6SPEC value.

2.4 Model formulation – water-stress-induced yield losses

The DO_3SE 3.1.0 model (Bland et al., 2025) was also used to model the effect of water stress on yield through the provision of estimates of potential (ET_m) and actual (ET_a) evapotranspiration following the DO_3SE model algorithms used to estimate soil–plant–atmosphere cycling of water as described in Büker et al. (2012). These DO_3SE algorithms essentially estimate the total loss of soil water through ET_a (and the equivalent ET_m) using the method of Shuttleworth and Wallace (1985), modified to incorporate the atmospheric, boundary layer, and stomatal resistances to water vapour flux as calculated within DO_3SE. Resistances are scaled from leaf to canopy using leaf area index (LAI) and upscaling methods described in Büker et al. (2012). LAI is modelled to vary over the course of the wheat-growing season between a value of 0 and 3.5 m^2 m^{-2} (consistently with average maximum LAI values frequently found across the IGP region,

Table 1. Modelled climate, [O_3], and [CO_2] data for the Varanasi grid box, used for the recent-past climate and both future RCP scenarios (expressed as a range of 24 h mean values; the value in brackets indicates the mean). The length of the growing season is shown in days over 2 years and can be seen in Fig. 2.

Parameter	Recent-past climate (1996–2005)	RCP4.5 (2046–2055)	RCP8.5 (2046–2055)
Temperature (°C)	17.4–20.6 (18.9)	19.1–21.3 (20.2)	19.6–21.8 (20.8)
VPD (hPa)	8.3–14.4 (11.0)	12.5–17.5 (14.5)	11.1–18.1 (15.1)
Precipitation (total over growing season; mm)	72.4–393.4 (235.5)	35.1–184.4 (101.7)	0.93–234.0 (92.5)
[O_3] (24 h mean; ppb)	47.1–50.6 (48.6)	57.9–62.2 (60.5)	54.6–63.0 (59.7)
[CO_2] (ppm)	362.6–379.5 (370.7)	476.3–498.5 (487.6)	518.6–570.5 (543.9)
Growing season (days over 2 years)	339–468	339–466	339–473

as observed from satellite data (Nigam et al., 2017)). The DO_3SE soil moisture module was developed based on the Penman–Monteith model of actual evapotranspiration (ET_a), which is described in Eq. (5) (Büker et al., 2012; Montieth, 1965; Shuttleworth and Wallace, 1985):

$$ET_a = \frac{\Delta(\Phi_n - G) + \rho_a c_p \left(\frac{D}{R_{bH_2O}}\right)}{\lambda\left\{\Delta + \gamma\left(1 + \frac{R_{stoH_2O}}{R_{bH_2O}}\right)\right\}}, \quad (5)$$

where Δ is the slope of the relationship between the saturation vapour pressure and temperature, Φ_n is the net radiation at the top of the canopy, G is the soil surface heat flux, ρ_a is the air density, c_p is the specific heat of air, D is the vapour pressure deficit of air, R_{bH_2O} is the canopy boundary layer resistance to water vapour exchange, R_{stoH_2O} is the stomatal canopy resistance to the transfer of water vapour (the inverse of stomatal conductance to water vapour), γ is the psychrometric constant, and λ is the latent heat of vaporisation.

The effect of ET_a (and, hence, water stress) on wheat yield was estimated according to the relationship between relative yield and the corresponding relative evapotranspiration (ET) described in Doorenbos and Kassam (1979) for spring wheat. When a crop is not water-stressed, ET_a is equal to ET_m; however, in drought conditions, $ET_a < ET_m$ (Yao, 1974). The ET_a and ET_m values produced by DO_3SE were used in Eq. (6).

$$1 - \frac{Y_a}{Y_m} = K_y\left(1 - \frac{ET_a}{ET_m}\right) \quad (6)$$

In the above, Y_a is the actual relative grain yield, and Y_m is the potential relative grain yield. K_y is the crop-specific yield response factor, assumed to be 1.15 for the whole growing season, in accordance with the value for spring wheat from the FAO (Steduto et al., 2012).

2.5 Model parameterisation

The DO_3SE model was parameterised for the HD-3118 and HUW-234 cultivars by Yadav et al. (2021) using data from a series of O_3 exposure experiments at the Banaras Hindu University, Varanasi, Uttar Pradesh. For this study, we use the same parameterisation, except for the f_{phen} term (which we allow to vary as a function of effective temperature sum (ETS) during the growing season) and the inclusion of the f_{O_3} term (which accounts for O_3 inducing early-onset senescence). The parameterisations used for both cultivars are given in Table 2.

The ETS model (see Eq. 7) was calibrated using experimental data for HUW-234 and HD-3118 that provided the timing (as day of year) of key crop development stages (sowing, emergence, flag leaf emergence, fully expanded flag leaf, start of seed setting, start of senescence and harvest) for both cultivars for 3 years (2016 to 2018 inclusive). Corresponding 3-hourly temperature data were used to estimate daily mean temperature from which ETS values could be determined according to Eq. (7).

$$ETS = \sum (T_i - T_b) \quad (7)$$

In the above, T_i is the mean daily temperature, and T_b is the base temperature, assumed to be 0 °C for wheat. This is equivalent to the method of thermal-time accumulation recommended by CLRTAP (2017) and assumes that there is no upper-threshold temperature for phenology and that thermal time increases linearly across the entire temperature range.

The ETS components of the f_{phen} function from flag leaf emergence were estimated by assuming that, together, $f_{phen}1\_ETS$ and $f_{phen}3\_ETS$ were equivalent to thermal time equally divided between the emerging flag leaf and seed setting. This precaution ensured that f_{phen} was not allowed to decrease too early; that $f_{phen}5\_ETS$ less $f_{phen}4\_ETS$ was equivalent to the thermal time at seed setting less the thermal time at flag leaf emergence; and that, together, $f_{phen}1\_ETS$ and $f_{phen}5\_ETS$ were equivalent to the thermal time at harvest less the thermal time at flag leaf emergence. These basic assumptions allowed for the derivation of f_{phen}_ETS parameters 1–5, given in Table 2. Fig. S1 in the Supplement gives an indication of the year-to-year variability in the timing of these key growth stages used to parameterise the f_{phen} function. This f_{phen} function is subsequently used to represent the phenological influence on g_{max} and to define the seasonal accumulation period for $POD_Y SPEC$ (see also CLRTAP (2017)). Parameterisation of the f_{phen}_ETS model

Table 2. Parameterisation of the DO_3SE model for POD_6SPEC for wheat flag leaves for Indian bread wheat (*Triticum aestivum* L.) cultivars. European bread wheat parameters reported by CLRTAP (2017) have been included for comparative purposes. Parameters are highlighted where there are differences between Indian and European cultivars.

Parameter	Units	Bread wheat cultivar parameterisation – POD_6SPEC		
		Indo-Gangetic Plains		Atlantic, boreal, continental
		HUW-234	HD-3118	bread wheat (CLRTAP, 2017)
g_{max}	mmol O_3 m^{-2} PLA s^{-1}	500	521	500
f_{min}	fraction	0.13	0.13	0.01
light_a	–	0.011	0.011	0.011
T_{min}	°	12	12	12
T_{opt}	°	26	26	26
T_{max}	°	40	40	40
VPD_{max}	kPa	3.2	3.2	1.2
VPD_{min}	kPa	4.6	4.6	3.2
$\sum VPD_{crit}$	kPa	16	16	8
PAW_t^*	%	50	50	50
f_{O_3}	POD_0 mmol O_3 m^{-2} PLA s^{-1}	14	14	14
Leaf dimension	cm	2	2	2
Canopy height	m	1	1	1
f_{phen_a}	fraction	0.3	0.3	0.3
f_{phen_e}	fraction	0.7	0.7	0.7
$f_{phen\_1\_ETS}$	°C d	−616.6	−553	−200
$f_{phen\_2\_ETS}$	°C d	0	0	0
$f_{phen\_3\_ETS}$	°C d	621.5	553	100
$f_{phen\_4\_ETS}$	°C d	182.75	238	525
$f_{phen\_5\_ETS}$	°C d	959	1000	700

* PAW_t is the threshold for plant available water (PAW) in millimetres, above which stomatal conductance is at a maximum.

shows little difference in terms of phenology between these cultivars, although HUW-234 had a greater range of dates of flag leaf emergence and fully expanded flag leaf. Seed setting and the start of senescence occurred ∼ 3 d earlier in HD-3118 than in HUW-234. The Indian cultivar f_{phen}_ETS values differ from the European continental bread wheat values (also shown in Table 2). In part, this is related to the precautionary approach taken in defining the length of the period during which f_{phen} will equal 1 to ensure that we capture the period when O_3 may be taken up by the stomata in the absence of growth stage data more specific to the f_{phen}_ETS stages. The resulting f_{phen}_ETS parameterisation suggests that Indian cultivars take more thermal time to reach mid-anthesis and less thermal time between the start of senescence and harvest than bread wheat from the European region would.

2.6 Model runs

DO_3SE 3.1.0 model (Bland et al., 2025) runs were made for each cultivar described in Table 2 using the WRF-Chem-modelled O_3 and meteorological data for 1996–2005, which was assumed to represent the recent-past climate. The DO_3SE model runs were repeated for future scenarios using the WRF-Chem-modelled O_3 and meteorological data for 2046–2055 based on the two scenarios of RCP4.5 and RCP8.5 to explore the influence of changes in climate and O_3 precursor emissions on O_3 uptake. We assume a sowing date of early November since October to December represent the main sowing months of wheat across the most productive wheat-growing states in the IGP (Lobell et al., 2013).

3 Results and discussion

3.1 Phenology and stomatal O_3 uptake

Accurate modelling of the growing season and the f_{phen} period in relation to the prevailing O_3 climate is crucial for realistic estimates of O_3 damage to wheat. The ETS model for late-sown cultivars is variable in its ability to simulate key growth stages between years and cultivars. For each growth stage, the minimum and maximum °C d values between years are 63 to 426 °C d for HUW-234 and 63 to 317°C d for HD-3118. Given that the mean daily temperature during the Indian wheat-growing season is ∼ 25 °C, this would suggest that the ETS model may have a maximum error of 17 and 13 d for HUW-234 and HD-3118, respectively. These values are likely to be at the high end of the uncertainty range as temperatures increase during the growing season, and the greatest uncertainty was found for the flag leaf emergence

and fully expanded flag leaf growth stages. The inclusion of the "emerging flag leaf" in the f_{phen} period helps to capture the full period when the flag leaf may be vulnerable to O_3 as a precaution given the uncertainty in the ETS model defining the timing of the period from full flag leaf expansion and senescence.

When the parameterisation was applied to the WRF-Chem-modelled 1996–2005 climate temperature data, with a sowing date of 5 November, maturity was simulated to occur around the end of March (consistently with our observed maturity date of the late-sown variety under the relatively high temperatures for the years 2016–2018, as used for parameterisation) – see Fig. 1. Thus, our f_{phen} parameterisation, when using standard early-November sowing dates, gives realistic maturity dates for the IGP region's grown wheat when used with recent-past WRF-Chem-modelled data (Fig. 2). Since the WRF-Chem data are consistent between climate periods (i.e. 1996–2005 and 2046–2055), they can be deemed to provide a means of comparing the relative effect of changes in temperature on the growing season, O_3 uptake, and the evolution of soil moisture deficit.

The empirical data used for model parameterisation collected in the years 2016–2018 consistently produced higher temperatures than the WRF-Chem model-based meteorological data, which were collected from 1996 to 2005 (Fig. 3a). This could be, in part, due to climate change; average air temperatures in India for 2016, 2017, and 2018 were in the top 10 on record since 1901 (India Meteorological Department, 2018). However, on average, the years of 2016, 201, and 2018 were only +0.72, +0.55, and +0.41 °C warmer than the 1981–2010 annual air temperature average, respectively (India Meteorological Department, 2018); therefore, it is likely that uncertainties in the modelled values caused the greater part of these discrepancies in temperatures. Since, at this resolution, the WRF-Chem model may not consider some urban heat island effects, a finer model resolution may have led to better agreement with observations for this urban site. Despite this, the nature of the ETS model is such that it can provide comparative estimates of the influence of temperature profiles on the timing and length of the growing season. Figure 3b shows a similar comparison between WRF-Chem-modelled O_3 concentrations (provided as 5-year mean hourly values, with absolute minimum and maximum bounds also shown) and the ambient-air (AA) O_3 concentration data for the 2016–2017 wheat-growing season of the O_3 experiment. This shows that the WRF-Chem-modelled past climate (1996–2005) data are within the range but at the lower end of the 2016–2017 O_3 experimental data, as would be expected given the increase in O_3 precursor emissions over the past few decades.

The DO_3SE wheat stomatal O_3 flux model has been evaluated against wheat g_{sto} data (the primary determinant of stomatal ozone flux) collected under experimental conditions in Ostad, Sweden (Pleijel et al., 2007), and was found to perform well (with an R^2 value of 0.83 for a regression of observed against modelled g_{sto}). The DO_3SE model has also been extensively evaluated for a number of crops at locations around the world (as reported in Tuovinen et al. (2004) for wheat growing near Comun Nuovo in Italy and in Emmerichs et al. (2025) for wheat growing near Grignon in France). These evaluations rely on total O_3 flux and deposition measurements (since they use O_3 flux tower data) or water vapour flux measurements and thereby test whole-canopy fluxes rather than the representative upper-leaf stomatal flux required for POD_Y calculations. However, the combination of these evaluation methods, focussing on both leaf-level g_{sto} and canopy-level O_3 flux, provides confidence in the predictive abilities of the DO_3SE model.

3.2 Effect of O_3 stress on the yield benefits of irrigation

Water-stress-induced yield loss under rainfed conditions modelled under the climate scenario for 1996–2005 was found to exceed O_3-relative yield loss (O_3-RYL) under irrigated conditions for the majority of the 10 years investigated. Under this climate, rainfed conditions produced a mean water-stress relative yield loss (WS-RYL) of 13.3 % for HUW-234, with a range of 2.8 %–31.3 % (Fig. 4a). Under rainfed conditions, the mean O_3-RYL was projected to be negligible (0.6 %), significantly lower than the mean O_3-RYL when no water stress is assumed under irrigation (10.7 %, with a range of 4.8 %–15.4 %). This demonstrates the importance of irrigation for wheat production in India and highlights the substantial influence on the yield of O_3 for irrigated wheat.

O_3-RYL under irrigated conditions exceeded WS-RYL in 80 % of the 10 years investigated in the RCP4.5 scenario (Fig. 4b). This highlights how O_3 stress negates some of the increased productivity that arises from reducing water stress through irrigation. In the RCP8.5 scenario, WS-RYL under rainfed conditions exceeded O_3-RYL under irrigated conditions in all but 1 year (2051), when precipitation totalled 234.0 mm for the growing season (Fig. 4c). In this scenario, precipitation during the growing season ranges from 0.9 to 234.0 mm, with a mean of 94 ± 82.97 mm, and, as a result, the WS-RYL fluctuates within the 10 years.

Whilst irrigation has played an important role in increasing yields for India's wheat, these results show that O_3 is likely to negate some of the yield benefits of irrigation. Based on the results of simulations of future climates, irrigation will have less of an effect on yield increases as $[O_3]$ levels rise.

The mean total precipitation for the growing season under the 1996–2005 climate scenario was higher than the median values in the RCP4.5 and RCP8.5 scenarios for 2046–2055, meaning that Uttar Pradesh's crops will receive less rainfall in the future. In addition, the RCP8.5 scenario had a larger interquartile range (IQR) of 131.0 mm than the 1996–2005 climate (54.8 mm) and the smallest lower quartile (22.3 mm), demonstrating less and more irregular precipitation in the future climate. Whilst RCP4.5 was less extreme, it had a larger

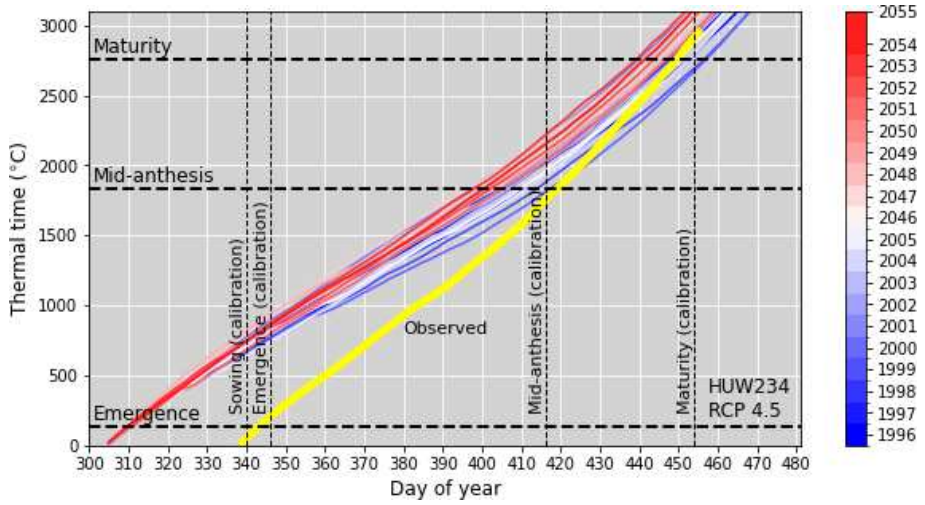

Figure 1. The evolution of ETS and associated growth stages for the observed (2016–2018) climate (based on which the ETS model is calibrated, with a sowing date of 5 December) and the WRF-Chem-modelled recent-past (1986–2005) and future (2046–2055; RCP4.5 and 8.0) climates (for which the model is applied, with a sowing date of 5 November) for the HUW-234 cultivar.

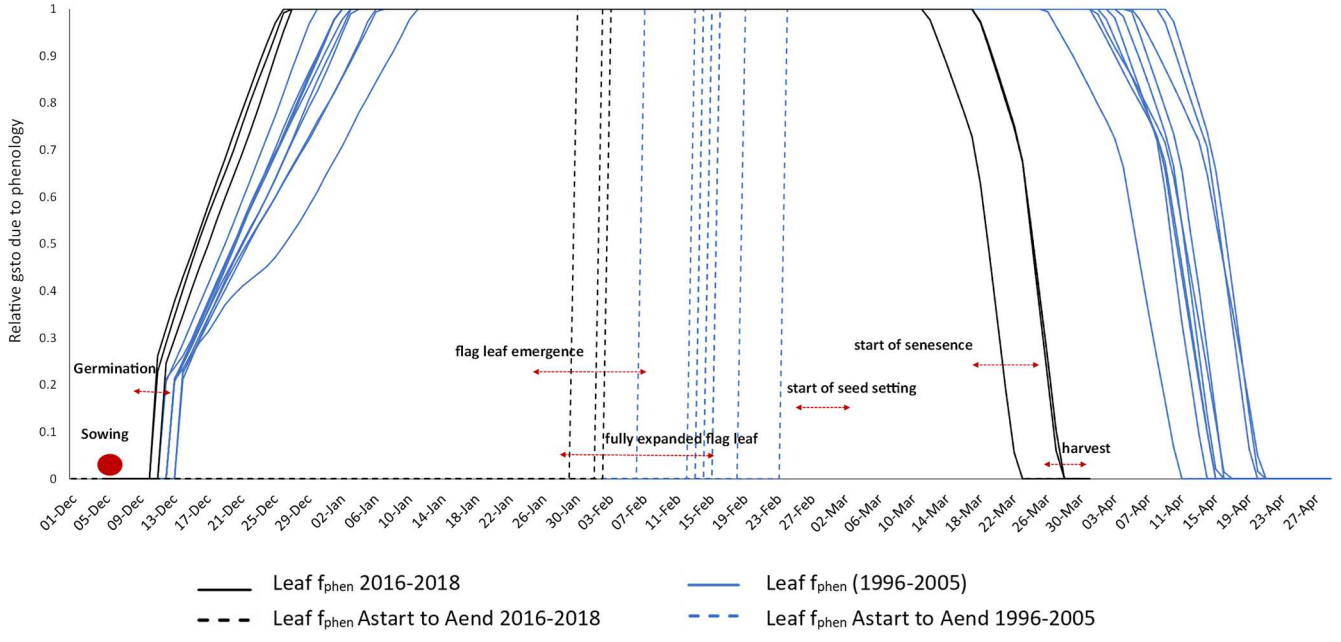

Figure 2. The ETS model parameterised for HUW-234 based on observed recent-past temperatures (2016–2018; black). The ETS model results for the modelled recent-past temperatures (years 1996–2005) are in blue. The ranges of observed dates of sowing, germination, flag leaf emergence, fully expanded flag leaf, start of seed setting, start of senescence, and harvest from the experimental data (D. S. Yadav, personal communication, 2020) are marked with arrows. Astart to Aend represent the start of anthesis to the end of anthesis.

IQR of 90.1 mm. This irregularity and increased risk of low precipitation over the growing season demonstrates the continuing importance of irrigation for wheat productivity. In all modelled climate scenarios, water stress tends to be a much greater threat to crop yields than O_3, and, therefore, some level of irrigation is crucial for sustained wheat productivity in India. However, these findings clearly show that O_3 is a limiting factor in relation to yield under irrigated conditions, meaning that the full potential benefit of irrigation is not being realised and, hence, will lead to inefficiencies in the use of irrigation water. Further research should be carried out to find the "sweet spot" for irrigation that will minimise O_3 stress without inducing water stress to practice more responsible water management.

Future studies should investigate how short, sharp high-O_3 periods could be mitigated with temporary reductions in irri-

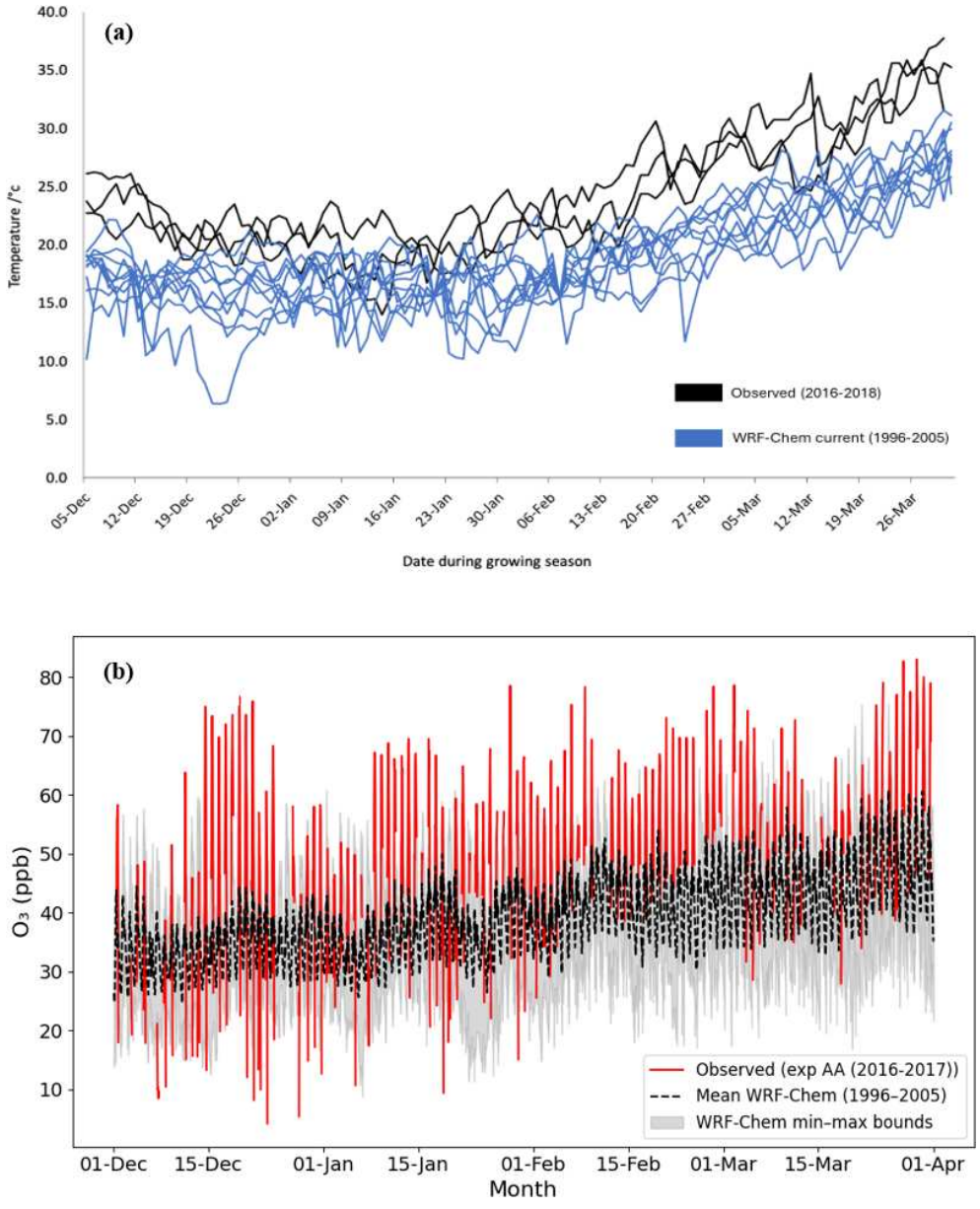

Figure 3. Seasonal profiles of **(a)** surface temperatures over the growing season for observed data (2016–2018) and WRF-Chem-modelled data for the recent-past climate (1996–2005) and **(b)** O_3 concentration over the growing season for observed data (exp AA (experiment ambient air)) for December 2016 to March 2017 and 10-year (1996–2005) annual mean WRF-Chem-modelled O_3 concentration data, with associated absolute minimum and maximum O_3 concentrations bounds also shown.

gation, and, if the efficacy of such approaches can be demonstrated, they could be practically applied in the future with the advent of new technologies such as accurate pollution forecasting via machine learning models (Jumin et al., 2020; Wang et al., 2020). A holistic approach that considers the trade-offs between other abiotic stressors such as heat stress is needed as irrigation plays a significant role in mitigating such stress (Zaveri and Lobell, 2019), and higher temperatures are a precursor of higher O_3 levels, with the chance that O_3 effects will be erroneously attributed to heat stress (Tai et al., 2014).

3.3 Effect of climate change on O_3 sensitivity

Higher O_3-induced yield losses were modelled under future scenarios (Fig. 5). For HUW234, a statistically significant increase in yield loss of $7.9 \pm 5.56\,\%$ and $3.1 \pm 5.08\,\%$ was modelled for RCP4.5 and RCP8.5, respectively, compared to the recent-past climate. Similarly, for RCP4.5 and RCP8.5,

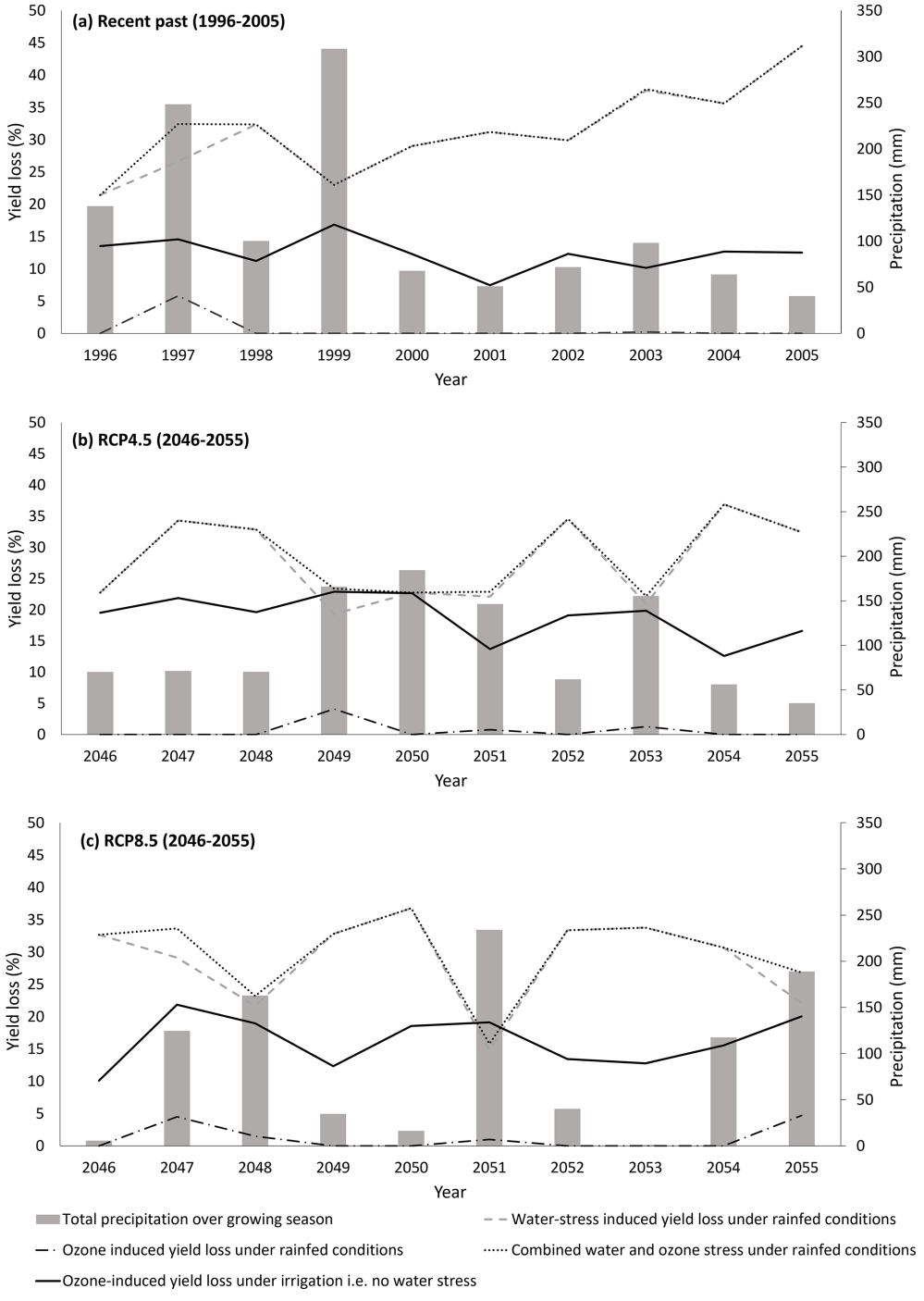

Figure 4. The water-stress- and ozone-related relative yield loss modelled for HUW-234 under rainfed conditions (water stress) and with no water stress (f_{sw} set to 1 in DO_3SE) for **(a)** the recent-past climate of 1996–2005, **(b)** the RCP4.5 scenario for 2046–2055, and **(c)** the RCP8.5 scenario for 2046–2055.

increases of 8.0 ± 5.71 % and 3.0 ± 4.87 % yield loss were predicted for HD-3118, respectively. This suggests that the increase in O_3 impact due to future emissions and/or climate is larger than the year-to-year variability in O_3 impact for the RCP4.5 scenario (but not for RCP8.5, where $[O_3]$ levels were lower; see below). The recent-past climate represents the lowest mean O_3, suggesting that O_3 – rather than other environmental conditions that might influence sensitivity to O_3 (i.e. via alterations to stomatal O_3 uptake) – is the most important factor in determining O_3-induced yield loss. These findings imply that the changing climate (i.e. higher frequency of temperatures that exceed T_{opt}, with consequent

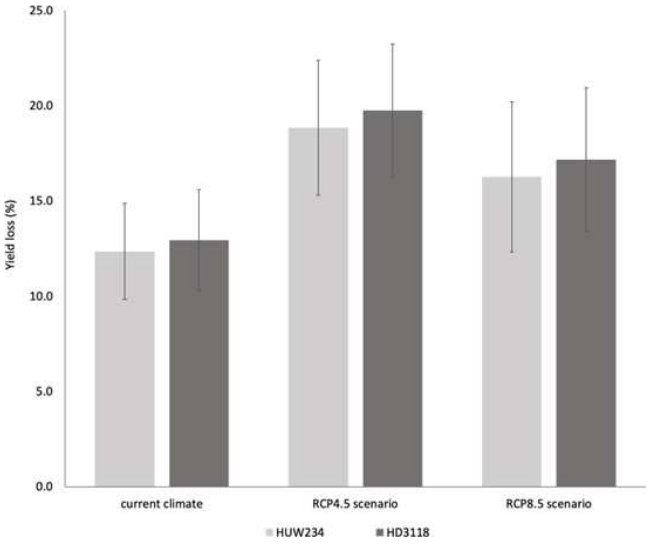

Figure 5. Mean O_3-induced relative yield losses (O_3-RYL) ±SD modelled for the recent-past climate (1996–2005) and two future climate scenarios for 2046–2055, namely RCP4.5 and RCP8.5, for two Indian spring wheat cultivars, namely HUW-234 and HD-3118.

reductions in stomatal conductance and, hence, O_3 flux) will be insufficient with regard to ameliorating the increase in O_3-induced yield loss. This contrasts with several studies that have shown the potential of elevated temperatures to lead to reductions in O_3 flux via reduced stomatal conductance, thus reducing O_3 damage (Emberson et al., 2018; Feng et al., 2008). This could be due to differences in the timing and duration of periods of more extreme temperatures that exist between studies, a possibility that would benefit from further study. It is important to clarify that, in this study, we explore future changes in ozone concentration due to changes in climate due to changes in O_3 precursor emissions. O_3 studies often explore the effect of a "climate change penalty", which is the impact of a future climate on O_3 levels if emissions are held constant (Wu et al., 2008; Zanis et al., 2022). Although this is not specifically investigated in this study, it is worth noting that India is one of the global regions with the strongest effect of a "climate change penalty" (Zanis et al 2022). Given the interplay between climate and O_3 in determining the extent of stomatal O_3 uptake and, hence, crop sensitivity to O_3, it is worth noting that, even without changes in emissions, O_3-induced crop damage would still be likely to change to some extent under future conditions.

The results from this study are within the range published by Mills et al. (2018b) for O_3-induced yield losses for wheat in Uttar Pradesh, which were modelled for 2010–2012 using POD_3IAM with a European wheat parameterisation and a broad-scale assessment of India's wheat-growing season. The Mills et al. (2018b) study used the most recent methodology from CLRTAP (2017) to calculate O_3-induced yield loss for wheat as a reference POD_3IAM value representing O_3 uptake at pre-industrial conditions was subtracted before crop loss was calculated. Whilst this study also uses a stomatal-flux-based metric, POD_3IAM is vegetation type specific, suitable for large-scale modelling (CLRTAP, 2017). The POD_6SPEC was used in this current study since we were able to define a cultivar-specific growth period with some certainty, thereby allowing greater confidence in the use of the more biologically relevant metric than POD_3IAM (CLRTAP, 2017). It is also worth noting that the timing of O_3 and water stress may be important in predicting how plants respond to these stresses since O_3 has been found to damage stomatal functioning, causing plants lose the ability to respond to water stress (e.g. Wilkinson et al., 2010). Ideally, O_3 impact models would include mechanisms that simulate O_3-induced loss in stomatal functioning; however, to our knowledge, such modelling mechanisms have not yet been developed or included and would likely require experimental data to identify thresholds at which stomatal functioning is impaired.

Mean relative O_3-induced yield losses for both cultivars modelled under RCP4.5 (18.7 ± 3.83 %) were significantly higher than those of RCP8.5 (13.8 ± 3.22 %). This is likely to be due to a combination of slightly higher [O_3] levels in RCP4.5 (Table 1) and the WRF-Chem model projections of higher temperatures (limiting O_3 flux as temperatures have a tendency to exceed T_{opt}) under RCP8.5. Whilst the RCP4.5 scenario sees a global reduction in [O_3] due to pollution regulation, the South Asian region is an exception to this rule, with [O_3] continuing to increase at a similar rate, as occurred in previous decades (Tai and Martin, 2017). RCP8.5 projects a worldwide increase in [O_3] due to the lack of regulation of precursor emissions, except in parts of the US and East and Southeast Asia (Tai and Martin, 2017). Therefore, mean [O_3] during the growing season is lowest in the recent-past climate at 48.6 ppb but is similar, at least in South Asia, in both the RCP4.5 and RCP8.5 scenarios (60.5 and 59.7 ppb, respectively; Table 1).

Relatively small differences in 2000–2050 increases in O_3 over South Asia between RCP4.5 and RCP8.5 have also been found before (Tai et al., 2014; their Fig. S1). Our WRF-Chem model results do show a slightly higher increase in O_3 precursors over India in RCP4.5 than in RCP8.5 (not shown), likely explaining the slightly higher O_3 increase in the RCP4.5 scenario. However, several factors influence the modelled future O_3 concentration changes, such as the future change in meteorological variables, the non-linearities of O_3 chemistry, and natural interannual variability. For example, Sharma et al. (2023) found underestimations of relative humidity in the meteorological data used in O_3 simulations, which will have some influence on O_3 production estimates. Future studies should utilise emission scenarios that are more updated in terms of air pollution policies.

The O_3-induced yield loss will increase from current levels, regardless of whether global emissions follow a business-as-usual or medium-stabilisation scenario. We predict that

O_3-induced yield losses will continue to increase in South Asia with climate change, given the co-emission of radiative forcers and O_3 precursors and the two-way causality that exists between O_3 formation and climate change; i.e. hot, sunny conditions, likely to be enhanced under climate change, encourage O_3 formation, whilst O_3 itself is a radiative forcer (Fu and Tian, 2019). This means that O_3 and climate variable stress are likely to co-occur in the future, which becomes especially problematic for crop productivity when environmental thresholds (e.g. due to temperature extremes) for plant productivity are exceeded. South Asia and the IGP are important agricultural regions where O_3 thresholds are currently being exceeded (Mills et al., 2018c), with the likelihood that the extent of such exceedance will only worsen in the future and with climate change (Cooper et al., 2014; Fowler et al., 2008; Fu and Tian, 2019; Rathore et al., 2023).

It should be noted that there are uncertainties in the WRF-Chem model used in modelling meteorological and [O_3] data. There are important criticisms that the WRF-Chem model is limited in its ability to capture true wind speeds, which influences temperature and O_3 mixing ratios (Rydsaa et al., 2016). Despite this, these findings serve as a useful insight into the future risk of O_3 to wheat yields relative to the conditions of the early 21st century. Ideally, future research should consider the use of model ensembles to more robustly capture ranges in future meteorological and [O_3] data.

3.4 Influence of cultivar physiology on O_3 sensitivity

The O_3-RYL results modelled for HUW-234 were similar to those for HD-3118 in the recent-past climate and in both the RCP4.5 and RCP8.5 scenarios (Fig. 5). This is due to the similarity in terms of g_{max} values for HUW-234 and HD-3118, which were estimated from empirical data to be 500 mmol O_3 m^{-2} PLA s^{-1} and 520.9 mmol O_3 m^{-2} PLA s^{-1}, respectively. The mean yield losses for recent-past climate and RCP scenarios combined, modelled for HD-3118 (14.5 ± 0.05 %), were similar to those for HUW-234 (14.3 ± 0.05 %), a difference of 0.2 %. Despite the similar mean yield losses observed for HD-3118 and HUW-234, these results align with concerns that modern wheat cultivars are more susceptible to O_3 damage as they are bred for maximum gas exchange or heat tolerance rather than O_3 tolerance (Emberson et al., 2018; Pleijel et al., 2006; Yadav et al., 2020). Typically, plant traits bred for heat tolerance and maximum gas exchange conflict with traits for O_3 tolerance and may increase irrigation requirements; i.e. higher stomatal conductance enhances transpiration rates, allowing for higher rates of photosynthesis (Pleijel et al., 2007; Yadav et al., 2020). Despite the potential for HD-3118 to produce higher yields due to a high stomatal conductance, HUW-234 performs better in terms of O_3 tolerance for Varanasi's recent-past conditions and projections for the future climate and [O_3]. This is also observed in the empirical data for Varanasi for the period of 2016–2018, which were used to parameterise the ETS model. The empirical data observed lower relative yield loss under elevated [O_3] compared to under ambient [O_3] for HUW-234 than for HD-3118 (21.2 % and 23.2 %, respectively; see Table S1 of the Supplement). Absolute yields failed to observe the higher yielding potential expected of HD-3118, even under ambient conditions; the mean absolute grain yield for HUW-234 under ambient [O_3] was 533.4 g m^{-1} compared to 432.8 g m^{-1} for HD-3118. Under elevated [O_3], the yield gap widens; HUW-234 has an absolute grain yield of 420.4 g m^{-1}, whilst HD-3118 has a yield of 332.3 g m^{-1}. This suggests that O_3 has a greater impact on yield in HD-3118 than in HUW-234, possibly even under ambient concentrations.

Despite corroborating literature for the DO_3SE model results (Yadav et al., 2020), there is some limitation in the ability to accurately parameterise the model for specific cultivars. Here, we have been able to parameterise key parameters that will influence stomatal O_3 flux (g_{max} and f_{phen}) for Indian varieties; however, the remaining parameters that determine the modification of g_{max} by environmental conditions rely on European parameterisations. Similarly, the DO_3SE model estimates O_3-induced crop yield losses based on a dose–response relationship configured using five European wheat cultivars (CLRTAP, 2017). Whilst the DO_3SE model is a valuable tool for risk assessment, the use of appropriately calibrated and evaluated crop models will provide mechanisms to fully explore the interplay between stresses such as O_3 and water stress on yield (Emberson et al., 2018). The results of this paper make clear the need for such modelling to improve our understanding of how these different stresses act over the course of the growing season to determine changes in productivity. A new generation of crop models that are being developed to incorporate the O_3 effect, as well as other stresses (Emberson et al., 2018), will be able to explore trade-offs between stresses related to soil water, extreme temperatures, and soil fertility. Such advances in crop modelling will be crucial in assessing future wheat productivity under a range of abiotic stress conditions.

In this Indian study, the mid-anthesis and grain-filling period occurred in March (Figs. 1 and 2), which corresponds to peak O_3 in Uttar Pradesh (Jain et al., 2023; Mukherjee et al., 2019; Shukla et al., 2017). However, a study on timely sown Chinese winter wheat cultivars found that elevated O_3 only had a significant effect during the mid-grain-filling stage, suggesting that timing mid-grain filling with O_3 troughs could be a mitigation strategy, which may be achieved by earlier sowing (Feng et al., 2016). Late planting results in reduced productivity of the wheat crop, with earlier, timely sowing of wheat in the third week of November yielding the best productivity in eastern Uttar Pradesh (Chandna et al., 2004). Past studies have reported that delays in sowing after mid-November lead to a reduction in the yield of wheat, often at a rate of 1 % d^{-1}–1.5 % d^{-1} (McDonald et al., 2022; Ortiz-Monasterio et al., 1994). In addition, Kumar et al. (2014) claimed that conversion from late

to timely sown would offset the impacts of climate change. A multi-tolerance approach like early sowing could mitigate heat and O_3 stress; however, late sowing is often due to delays in harvesting rice in rice–wheat systems, a cropping sequence which provides income for tens of millions of farm families (Jain et al., 2017; Mishra et al., 2021). Further investigation of the interplay between [O_3] profiles over the growing season and targeted crop phenology of different cultivar types should be conducted.

4 Conclusion

Whilst irrigation has played a pivotal role in increasing wheat production in India through maximising yields, O_3 is likely to negate some of the yield benefits of irrigation, which will reduce irrigation efficiency. Based on the POD_6SPEC values obtained via the DO_3SE model and associated flux–response relationships, O_3 concentrations prevalent in the IGP region of India are high enough to cause grain yield losses in Indian wheat. This paper demonstrates the complexity of avoiding O_3 stress and the importance of taking a multi-stress approach to mitigation. Since high levels of O_3 typically coincide with other abiotic stressors, such as heat stress, the approach taken to maximise crop yield must consider multiple stressors and their interactions. Rather than altering irrigation patterns to mitigate O_3 stress and risk increasing the effect of other stressors such as water stress or heat stress, earlier sowing to avoid peak O_3 and temperatures in March may benefit irrigated wheat growing in India. Given that modern wheat cultivars are more O_3 sensitive, wheat growers should reconsider using modern cultivars bred for optimal gas exchange.

Code availability. An open version of the DO3SE model code, release 3.1.0 DO3SE/DO3SE-UI: v3.1.0, as used in the present study can be found at https://doi.org/10.5281/zenodo.16752474 (Bland et al., 2025).

Data availability. Experimental data from https://doi.org/10.1016/j.envpol.2020.113939 (Yadav et al., 2020) and https://doi.org/10.1016/j.fcr.2021.108076 (Yadav et al., 2021) were used in the present study with additional data provided by Durgesh Singh Yadav (durgeshsinghy@gmail.com). Due to data ownership, please contact Durgesh Singh Yadav directly for access to required experimental data.

WRFChem modelled data will be made available upon request.

Supplement. The supplement related to this article is available online at https://doi.org/10.5194/bg-22-4203-2025-supplement.

Author contributions. GE and LE designed the modelling study, and GE and SB performed the DO_3SE model runs. OH provided the modelled O_3 and meteorological data and advised on their use within the study. MA and DSY provided the experimental data used to calibrate the DO_3SE model and advised on their use within the study. CON, CJ, JC, and PP supported DO_3SE model calibration and analysis of the results. GE prepared the paper with contributions from all of the co-authors.

Competing interests. The contact author has declared that none of the authors has any competing interests.

Disclaimer. Publisher's note: Copernicus Publications remains neutral with regard to jurisdictional claims made in the text, published maps, institutional affiliations, or any other geographical representation in this paper. While Copernicus Publications makes every effort to include appropriate place names, the final responsibility lies with the authors.

Special issue statement. This article is part of the special issue "Tropospheric Ozone Assessment Report Phase II (TOAR-II) Community Special Issue (ACP/AMT/BG/GMD inter-journal SI)". It is a result of the Tropospheric Ozone Assessment Report, Phase II (TOAR-II, 2020–2024).

Acknowledgements. The Viking cluster was used during this project; this is a high-performance-computing facility provided by the University of York. We are grateful for the support of the University of York, their IT services, and their research IT team.

Financial support. Funding from The Norwegian Research Council CICERO strategic project (grant no. 160015/F40) and the CiX-PAG project (grant no. 244551) provided support to Lisa Emberson, Øivind Hodnebrog, and Madhoolika Agrawal.

Review statement. This paper was edited by Paul Stoy and reviewed by two anonymous referees.

References

Ainsworth, E. A., Rogers, A., and Leakey, A. D. B.: Targets for crop biotechnology in a future high-CO_2 and high-O_3 world, Plant Physiol., 147, 13–19, https://doi.org/10.1104/pp.108.117101, 2008.

Ali, M., Jensen, C. R., Mogensen, V. O., Andersen, M. N., and Henson, I. E.: Root signalling and osmotic adjustment during intermittent soil drying sustain grain yield of field grown wheat, F. Crop. Res., 62, 35–52, https://doi.org/10.1016/S0378-4290(99)00003-9, 1999.

Bland, S., Briolat, A., and Gillies, D.: DO3SE/DO3SE-UI: v3.1.0 (release-3.1.0), Zenodo [data set], https://doi.org/10.5281/zenodo.16752474, 2025.

Broberg, M. C., Hayes, F., Harmens, H., Uddling, J., Mills, G., and Pleijel, H.: Effects of ozone, drought and heat stress on wheat yield and grain quality, Agr. Ecosyst. Environ., 352, 108505, https://doi.org/10.1016/j.agee.2023.108505, 2023.

Büker, P., Morrissey, T., Briolat, A., Falk, R., Simpson, D., Tuovinen, J.-P., Alonso, R., Barth, S., Baumgarten, M., Grulke, N., Karlsson, P. E., King, J., Lagergren, F., Matyssek, R., Nunn, A., Ogaya, R., Peñuelas, J., Rhea, L., Schaub, M., Uddling, J., Werner, W., and Emberson, L. D.: DO_3SE modelling of soil moisture to determine ozone flux to forest trees, Atmos. Chem. Phys., 12, 5537–5562, https://doi.org/10.5194/acp-12-5537-2012, 2012.

Chandna, P., Hodson, D. P., Singh, U. P., Singh, A. N., Gosain, A. K., Sahoo, R. N., and Gupta, R. K.: Increasing the Productivity of Underutilized Lands by Targeting Resource Conserving Technologies-A GIS/Remote Sensing Approach: A Case Study of Ballia District, Uttar Pradesh, in the Eastern Gangentic Plains, CIMMYT, 43 pp., ISBN 970-648-118-4, 2004.

CLRTAP: Mapping critical levels for vegetation, in: Manual on methodologies and criteria for modelling and mapping critical loads and levels and air pollution effects, risks and trends, https://icpvegetation.ceh.ac.uk/sites/default/files/FinalnewChapter3v4Oct2017_000.pdf (last access: 22 July 2025), 2017.

Conway, T. J.: Global mean growth rates, https://data.giss.nasa.gov/modelforce/ghgases/Fig1A.ext.txt, last access: 8 February 2020.

Cooper, O. R., Parrish, D. D., Ziemke, J., Balashov, N. V., Cupeiro, M., Galbally, I. E., Gilge, S., Horowitz, L., Jensen, N. R., Lamarque, J. F., Naik, V., Oltmans, S. J., Schwab, J., Shindell, D. T., Thompson, A. M., Thouret, V., Wang, Y., and Zbinden, R. M.: Tropospheric Ozone Assessment Report: Global distribution and trends of tropospheric ozone: An observation-based review, Elem. Sci. Anthr., 2, 1–28, https://doi.org/10.12952/journal.elementa.000029, 2014.

Daloz, A. S., Rydsaa, J. H., Hodnebrog, Sillmann, J., van Oort, B., Mohr, C. W., Agrawal, M., Emberson, L., Stordal, F., and Zhang, T.: Direct and indirect impacts of climate change on wheat yield in the Indo-Gangetic plain in India, J. Agr. Food Res., 4, 100132, https://doi.org/10.1016/j.jafr.2021.100132, 2021.

Deb Roy, S., Beig, G., and Ghude, S. D.: Exposure-plant response of ambient ozone over the tropical Indian region, Atmos. Chem. Phys., 9, 5253–5260, https://doi.org/10.5194/acp-9-5253-2009, 2009.

Doorenbos, J. and Kassam, A. H.: Crop yield response to water, FAO Irrig. Drain. Pap. no. 33, 33, ISBN 92-5-100744-6, 1979.

Emberson, L. D., Ashmore, M. R., Cambridge, H. M., Simpson, D., and Tuovinend, J.: Modelling stomatal ozone flux across Europe, Environ. Pollut., 109, 403–413, 2000a.

Emberson, L. D., Simpson, D., Tuovinen, J., Ashmore, M. R., and Cambridge, H. M.: Towards a model of ozone deposition and stomatal uptake over Europe, in: Research Note No. 42, EMEP/MSC-W 6/2000, ISSN 0332-9879, Norwegian Meteorological Institute, 2000b.

Emberson, L. D., Pleijel, H., Ainsworth, E. A., van den Berg, M., Ren, W., Osborne, S., Mills, G., Pandey, D., Dentener, F., Büker, P., Ewert, F., Koeble, R., and Van Dingenen, R.: Ozone effects on crops and consideration in crop models, Eur. J. Agron., 100, 19–34, https://doi.org/10.1016/j.eja.2018.06.002, 2018.

Emmerichs, T., Al Mamun, A., Emberson, L., Mao, H., Zhang, L., Ran, L., Betancourt, C., Wong, A., Koren, G., Gerosa, G., Huang, M., and Guaita, P.: Can atmospheric chemistry deposition schemes reliably simulate stomatal ozone flux across global land covers and climates?, EGUsphere [preprint], https://doi.org/10.5194/egusphere-2025-429, 2025.

Fangmeier, A., Brockerhoff, U., Grüters, U., and Jäger, H. J.: Growth and yield responses of spring wheat (*Triticum aestivum* L. CV. Turbo) grown in open-top chambers to ozone and water stress, Environ. Pollut., 83, 317–325, https://doi.org/10.1016/0269-7491(94)90153-8, 1994.

Farooq, M., Hussain, M., and Siddique, K. H. M.: Drought Stress in Wheat during Flowering and Grain-filling Periods, Crit. Rev. Plant Sci., 33, 331–349, https://doi.org/10.1080/07352689.2014.875291, 2014.

Feng, Z., Kobayashi, K., and Ainsworth, E. A.: Impact of elevated ozone concentration on growth, physiology, and yield of wheat (*Triticum aestivum* L.): A meta-analysis, Glob. Change Biol., 14, 2696–2708, https://doi.org/10.1111/j.1365-2486.2008.01673.x, 2008.

Feng, Z., Wang, L., Pleijel, H., Zhu, J., and Kobayashi, K.: Differential effects of ozone on photosynthesis of winter wheat among cultivars depend on antioxidative enzymes rather than stomatal conductance, Sci. Total Environ., 572, 404–411, https://doi.org/10.1016/j.scitotenv.2016.08.083, 2016.

Fischer, G., Tubiello, F. N., van Velthuizen, H., and Wiberg, D. A.: Climate change impacts on irrigation water requirements: Effects of mitigation, 1990–2080, Technol. Forecast. Soc., 74, 1083–1107, https://doi.org/10.1016/j.techfore.2006.05.021, 2007.

Fishman, R.: Groundwater depletion limits the scope for adaptation to increased rainfall variability in India, Clim. Change, 147, 195–209, https://doi.org/10.1007/s10584-018-2146-x, 2018.

Fowler, D., Amann, M., Anderson, R., Ashmore, M., Cox, P., Depledge, M., Derwent, D., Grennfelt, P., Hewitt, N., Hov, O., Jenkin, M., Kelly, F., Liss, P., Pilling, M., Pyle, J., Slingo, J., and Stevenson, D.: Ground-level ozone in the 21st century: future trends, impacts and policy implications, 134 pp., The Royal Society, ISBN 978-0-85403-713-1, 2008.

Fu, T. M. and Tian, H.: Climate Change Penalty to Ozone Air Quality: Review of Current Understandings and Knowledge Gaps, Curr. Pollut. Reports, 5, 159–171, https://doi.org/10.1007/s40726-019-00115-6, 2019.

Gelang, J., Pleijel, H., Sild, E., Danielsson, H., Younis, S., and Selldén, G.: Rate and duration of grain filling in relation to flag leaf senescence and grain yield in spring wheat (*Triticum aestivum*) exposed to different concentrations of ozone, Physiol. Plant., 110, 366–375, https://doi.org/10.1111/j.1399-3054.2000.1100311.x, 2000.

Gent, P. R., Danabasoglu, G., Donner, L. J., Holland, M. M., Hunke, E. C., Jayne, S. R., Lawrence, D. M., Neale, R. B., Rasch, P. J., Vertenstein, M., Worley, P. H., Yang, Z. L., and Zhang, M.: The community climate system model version 4, J. Climate, 24, 4973–4991, https://doi.org/10.1175/2011JCLI4083.1, 2011.

Ghosh, A., Agrawal, M., and Agrawal, S. B.: Effect of water deficit stress on an Indian wheat cultivar (*Triticum aestivum* L. HD 2967) under ambient and elevated level of ozone, Sci. Total Environ., 714, 136837, https://doi.org/10.1016/j.scitotenv.2020.136837, 2020.

Ghude, S. D., Jena, C., Chate, D. M., Beig, G., Pfister, G. G., Kumar, R., and Ramanathan, V.: Reductions in India's crop yield due to ozone, Geophys. Res. Lett., 41, 5685–5691, https://doi.org/10.1002/2014GL060930, 2014.

Grell, G. A., Peckham, S. E., Schmitz, R., McKeen, S. A., Frost, G., Skamarock, W. C., and Eder, B.: Fully coupled "online" chemistry within the WRF model, Atmos. Environ., 39, 6957–6975, https://doi.org/10.1016/j.atmosenv.2005.04.027, 2005.

Harmens, H., Hayes, F., Sharps, K., Radbourne, A., and Mills, G.: Can reduced irrigation mitigate ozone impacts on an ozone-sensitive african wheat variety?, Plants, 8, 220, https://doi.org/10.3390/plants8070220, 2019.

He, C. and Zhou, T.: Responses of the western North Pacific subtropical high to global warming under RCP4.5 and RCP8.5 scenarios projected by 33 CMIP5 models: The dominance of tropical Indian Ocean-tropical western Pacific SST gradient, J. Climate, 28, 365–380, https://doi.org/10.1175/JCLI-D-13-00494.1, 2015.

Hodnebrog, O., Marelle, L., Alterskjær, K., Wood, R. R., Ludwig, R., Fischer, E. M., Richardson, T. B., Forster, P. M., Sillmann, J., and Myhre, G.: Intensification of summer precipitation with shorter time-scales in Europe, Environ. Res. Lett., 14, 124050, https://doi.org/10.1088/1748-9326/ab549c, 2019.

India Meteorological Department: 2018 Annual Climate Report, https://metnet.imd.gov.in/docs/imdnews/ANNUAL_REPORT2018English.pdf (last access:22 July 2025), 2018.

Jain, M., Singh, B., Srivastava, A. A. K., Malik, R. K., McDonald, A. J., and Lobell, D. B.: Using satellite data to identify the causes of and potential solutions for yield gaps in India's Wheat Belt, Environ. Res. Lett., 12, 094011, https://doi.org/10.1088/1748-9326/aa8228, 2017.

Jain, V., Tripathi, N., Tripathi, S. N., Gupta, M., Sahu, L. K., Murari, V., Gaddamidi, S., Shukla, A. K., and Prevot, A. S. H.: Real-time measurements of non-methane volatile organic compounds in the central Indo-Gangetic basin, Lucknow, India: source characterisation and their role in O_3 and secondary organic aerosol formation, Atmos. Chem. Phys., 23, 3383–3408, https://doi.org/10.5194/acp-23-3383-2023, 2023.

Joshi, A. K., Chand, R., Arun, B., Singh, R. P., and Ortiz, R.: Breeding crops for reduced-tillage management in the intensive, rice-wheat systems of South Asia, Euphytica, 153, 135–151, https://doi.org/10.1007/s10681-006-9249-6, 2007.

Jumin, E., Zaini, N., Ahmed, A. N., Abdullah, S., Ismail, M., Sherif, M., Sefelnasr, A., and El-Shafie, A.: Machine learning versus linear regression modelling approach for accurate ozone concentrations prediction, Eng. Appl. Comp. Fluid, 14, 713–725, https://doi.org/10.1080/19942060.2020.1758792, 2020.

Kangasjärvi, J., Jaspers, P., and Kollist, H.: Signalling and cell death in ozone-exposed plants, Plant Cell Environ., 28, 1021–1036, https://doi.org/10.1111/j.1365-3040.2005.01325.x, 2005.

Khan, S. and Soja, G.: Yield responses of wheat to zone exposure as modified by drought-induced differences in ozone uptake, Water. Air. Soil Poll., 147, 299–315, https://doi.org/10.1023/A:1024577429129, 2003.

Kumar, S. N., Aggarwal, P. K., Swaroopa Rani, D. N., Saxena, R., Chauhan, N., and Jain, S.: Vulnerability of wheat production to climate change in India, Clim. Res., 59, 173–187, https://doi.org/10.3354/cr01212, 2014.

Lamarque, J.-F., Bond, T. C., Eyring, V., Granier, C., Heil, A., Klimont, Z., Lee, D., Liousse, C., Mieville, A., Owen, B., Schultz, M. G., Shindell, D., Smith, S. J., Stehfest, E., Van Aardenne, J., Cooper, O. R., Kainuma, M., Mahowald, N., McConnell, J. R., Naik, V., Riahi, K., and van Vuuren, D. P.: Historical (1850–2000) gridded anthropogenic and biomass burning emissions of reactive gases and aerosols: methodology and application, Atmos. Chem. Phys., 10, 7017–7039, https://doi.org/10.5194/acp-10-7017-2010, 2010.

Lamarque, J. F., Kyle, P. P., Meinshausen, M., Riahi, K., Smith, S. J., van Vuuren, D. P., Conley, A. J., and Vitt, F.: Global and regional evolution of short-lived radiatively-active gases and aerosols in the Representative Concentration Pathways, Climatic Change, 109, 191–212, https://doi.org/10.1007/s10584-011-0155-0, 2011.

Lobell, D. B., Ortiz-Monasterio, J. I., Sibley, A. M., and Sohu, V. S.: Satellite detection of earlier wheat sowing in India and implications for yield trends, Agr. Syst., 115, 137–143, https://doi.org/10.1016/j.agsy.2012.09.003, 2013.

McDonald, A. J., Balwinder-Singh, Keil, A., Srivastava, A., Craufurd, P., Kishore, A., Kumar, V., Paudel, G., Singh, S., Singh, A. K., Sohane, R. K., and Malik, R. K.: Time management governs climate resilience and productivity in the coupled rice–wheat cropping systems of eastern India, Nat. Food, 3, 542–551, https://doi.org/10.1038/s43016-022-00549-0, 2022.

Meinshausen, M., Smith, S. J., Calvin, K., Daniel, J. S., Kainuma, M. L. T., Lamarque, J., Matsumoto, K., Montzka, S. A., Raper, S. C. B., Riahi, K., Thomson, A., Velders, G. J. M., and van Vuuren, D. P. P.: The RCP greenhouse gas concentrations and their extensions from 1765 to 2300, Climatic Change, 109, 213–241, https://doi.org/10.1007/s10584-011-0156-z, 2011.

Mills, G., Sharps, K., Simpson, D., Pleijel, H., Frei, M., Burkey, K., Emberson, L., Uddling, J., Broberg, M., Feng, Z., Kobayashi, K., and Agrawal, M.: Closing the global ozone yield gap: Quantification and cobenefits for multistress tolerance, Glob. Change Biol., 24, 4869–4893, https://doi.org/10.1111/gcb.14381, 2018a.

Mills, G., Sharps, K., Simpson, D., Pleijel, H., Broberg, M., Uddling, J., Jaramillo, F., Davies, W. J., Dentener, F., Van den Berg, M., Agrawal, M., Agrawal, S. B., Ainsworth, E. A., Büker, P., Emberson, L., Feng, Z., Harmens, H., Hayes, F., Kobayashi, K., Paoletti, E., and Van Dingenen, R.: Ozone pollution will compromise efforts to increase global wheat production, Glob. Change Biol., 24, 3560–3574, https://doi.org/10.1111/gcb.14157, 2018b.

Mills, G., Pleijel, H., Malley, C. S., Sinha, B., Cooper, O. R., Schultz, M. G., Neufeld, H. S., Simpson, D., Sharps, K., Feng, Z., Gerosa, G., Harmens, H., Kobayashi, K., Saxena, P., Paoletti, E., Sinha, V., and Xu, X.: Tropospheric Ozone Assessment Report: Present-day ozone distribution and trends relevant to human health, Elem. Sci. Anthr., 6, 47, https://doi.org/10.1525/elementa.302, 2018c.

Ministry of Agriculture & Farmers Welfare: Agricultural Statistics at a Glance 2021, New Delhi, 431 pp., https://desagri.gov.in/wp-content/uploads/2021/07/Agricultural-Statistics-at-a-Glance-2021-English-version.pdf (last access: 22 July 2025), 2022.

Mishra, J. S., Poonia, S. P., Kumar, R., Dubey, R., Kumar, V., Mondal, S., Dwivedi, S. K., Rao, K. K., Kumar, R., Tamta, M., Verma, M., Saurabh, K., Kumar, S., Bhatt, B. P., Malik, R. K., McDonald, A., and Bhaskar, S.: An impact of agronomic prac-

tices of sustainable rice-wheat crop intensification on food security, economic adaptability, and environmental mitigation across eastern Indo-Gangetic Plains, Field Crop. Res., 267, 108164, https://doi.org/10.1016/j.fcr.2021.108164, 2021.

Montieth, J. L.: Evaporation and environment, Symp. Soc. Exp. Biol., 19, 205–234, 1965.

Morgan, J. M.: Osmoregulation and Water Stress in Higher Plants, Annu. Rev. Plant Phys., 35, 299–319, https://doi.org/10.1146/annurev.pp.35.060184.001503, 1984.

Mukherjee, A., Wang, S. Y. S., and Promchote, P.: Examination of the climate factors that reduced wheat yield in northwest India during the 2000s, Water, 11, 1–13, https://doi.org/10.3390/w11020343, 2019.

Nigam, R., Vyas, S. S., Bhattacharya, B. K., Oza, M. P., and Manjunath, K. R.: Retrieval of regional LAI over agricultural land from an Indian geostationary satellite and its application for crop yield estimation, J. Spat. Sci., 62, 103–125, https://doi.org/10.1080/14498596.2016.1220872, 2017.

Ortiz-Monasterio, R., J. I. Ortiz-Monasterio, R., Dhillon, S. S., and Fischer, R. A.: Date of sowing effects on grain yield and yield components of irrigated spring wheat cultivars and relationships with radiation and temperature in Ludhiana, India, F. Crop. Res., 37, 169–184, https://doi.org/10.1016/0378-4290(94)90096-5, 1994.

Pleijel, H., Danielsson, H., Gelang, J., Sild, E., and Selldén, G.: Growth stage dependence of the grain yield response to ozone in spring wheat (*Triticum aestivum* L.), Agr. Ecosyst. Environ., 70, 61–68, https://doi.org/10.1016/S0167-8809(97)00167-9, 1998.

Pleijel, H., Eriksen, A. B., Danielsson, H., Bondesson, N., and Selldén, G.: Differential ozone sensitivity in an old and a modern Swedish wheat cultivar – Grain yield and quality, leaf chlorophyll and stomatal conductance, Environ. Exp. Bot., 56, 63–71, https://doi.org/10.1016/j.envexpbot.2005.01.004, 2006.

Pleijel, H., Danielsson, H., Emberson, L., Ashmore, M. R., and Mills, G.: Ozone risk assessment for agricultural crops in Europe: Further development of stomatal flux and flux-response relationships for European wheat and potato, Atmos. Environ., 41, 3022–3040, https://doi.org/10.1016/j.atmosenv.2006.12.002, 2007.

Rathore, A., Gopikrishnan, G. S., and Kuttippurath, J.: Changes in tropospheric ozone over India: Variability, long-term trends and climate forcing, Atmos. Environ., 309, 119959, https://doi.org/10.1016/j.atmosenv.2023.119959, 2023.

Riahi, K., Rao, S., Krey, V., Cho, C., Chirkov, V., Fischer, G., Kindermann, G., Nakicenovic, N., and Rafaj, P.: RCP 8.5-A scenario of comparatively high greenhouse gas emissions, Climatic Change, 109, 33–57, https://doi.org/10.1007/s10584-011-0149-y, 2011.

Roy, S., Beig, G., and Jacob, D.: Seasonal distribution of ozone and its precursors over the tropical Indian region using regional chemistry-transport model, J. Geophys. Res.-Atmos., 113, D21307, https://doi.org/10.1029/2007JD009712, 2008.

Rydsaa, J. H., Stordal, F., Gerosa, G., Finco, A., and Hodnebrog: Evaluating stomatal ozone fluxes in WRF-Chem: Comparing ozone uptake in Mediterranean ecosystems, Atmos. Environ., 143, 237–248, https://doi.org/10.1016/j.atmosenv.2016.08.057, 2016.

Sharma, A., Ojha, N., Pozzer, A., Mar, K. A., Beig, G., Lelieveld, J., and Gunthe, S. S.: WRF-Chem simulated surface ozone over south Asia during the pre-monsoon: effects of emission inventories and chemical mechanisms, Atmos. Chem. Phys., 17, 14393–14413, https://doi.org/10.5194/acp-17-14393-2017, 2017.

Sharma, A., Ojha, N., Pozzer, A., Beig, G., and Gunthe, S. S.: Revisiting the crop yield loss in India attributable to ozone, Atmos. Environ. X, 1, 100008, https://doi.org/10.1016/j.aeaoa.2019.100008, 2019.

Sharma, A., Venkataraman, C., Muduchuru, K., Singh, V., Kesarkar, A., Ghosh, S., and Dey, S.: Aerosol radiative feedback enhances particulate pollution over India: A process understanding, Atmos. Environ., 298, 119609, https://doi.org/10.1016/j.atmosenv.2023.119609, 2023.

Shukla, K., Srivastava, P. K., Banerjee, T., and Aneja, V. P.: Trend and variability of atmospheric ozone over middle Indo-Gangetic Plain: impacts of seasonality and precursor gases, Environ. Sci. Pollut. R., 24, 164–179, https://doi.org/10.1007/s11356-016-7738-2, 2017.

Shuttleworth, W. J. and Wallace, J. S.: Evaporation from sparse crops-an energy combination theory, Q. J. Roy. Meteor. Soc., 111, 839–855, 1985.

Singh, A. A. and Agrawal, S. B.: Tropospheric ozone pollution in India: effects on crop yield and product quality, Environ. Sci. Pollut. R., 24, 4367–4382, https://doi.org/10.1007/s11356-016-8178-8, 2017.

Steduto, P., Hsiao, T. C., Fereres, E., and Raes, D.: Crop yield response to water, FAO Irrigation and Drainage Paper no. 66, FAO, ISBN 978-92-5-107274-5, 2012.

Stockwell, W. R., Middleton, P., Chang, J. S., and Tang, X.: The second generation regional acid deposition model chemical mechanism for regional air quality modeling, J. Geophys. Res.-Atmos., 95, 16343–16367, https://doi.org/10.1029/JD095iD10p16343, 1990.

Tai, A. P. K. and Martin, M. V.: Impacts of ozone air pollution and temperature extremes on crop yields: Spatial variability, adaptation and implications for future food security, Atmos. Environ., 169, 11–21, https://doi.org/10.1016/j.atmosenv.2017.09.002, 2017.

Tai, A. P. K., Martin, M. V., and Heald, C. L.: Threat to future global food security from climate change and ozone air pollution, Nat. Clim. Change, 4, 817–821, https://doi.org/10.1038/nclimate2317, 2014.

Tans, P. P. and Conway, T. J.: Global means constructed using about 70 CMDL CCGG Sampling Network station data, https://data.giss.nasa.gov/modelforce/ghgases/Fig1A.ext.txt, last access: 8 February 2020.

Teixeira, E., Fischer, G., van Velthuizen, H., van Dingenen, R., Dentener, F., Mills, G., Walter, C., and Ewert, F.: Limited potential of crop management for mitigating surface ozone impacts on global food supply, Atmos. Environ., 45, 2569–2576, https://doi.org/10.1016/j.atmosenv.2011.02.002, 2011.

Tripathi, A. and Mishra, A. K.: The Wheat Sector in India: Production, Policies and Food Security, in: The Eurasian Wheat Belt and Food Security: Global and Regional Aspects, 275–296, https://doi.org/10.1007/978-3-319-33239-0_17, 2017.

Tuovinen, J.-P., Ashmore, M. R., Emberson, L. D. and Simpson, D.: Testing and improving the EMEP ozone deposition model, Atmos. Environ., 38, 2373–2385, https://doi.org/10.1016/j.atmosenv.2004.01.026, 2004.

UNDESA (United Nations Department of Economic and Social Affairs): World Population Prospects 2022: Summary of Results, UN DESA/POP/2-22/TR/NO.3, https://www.un.org/development/desa/pd/sites/www.un.org.development.desa.pd/files/undesa_pd_2022_wpp_key-messages.pdf (last access: 22 July 2025), 2022.

van Vuuren, D. P., Edmonds, J., Kainuma, M., Riahi, K., Thomson, A., Hibbard, K., Hurtt, G. C., Kram, T., Krey, V., Lamarque, J. F., Masui, T., Meinshausen, M., Nakicenovic, N., Smith, S. J., and Rose, S. K.: The representative concentration pathways: An overview, Climatic Change, 109, 5–31, https://doi.org/10.1007/s10584-011-0148-z, 2011.

Wada, Y., Wisser, D., Eisner, S., Flörke, M., Gerten, D., Haddeland, I., Hanasaki, N., Masaki, Y., Portmann, F. T., Stacke, T., Tessler, Z., and Schewe, J.: Multimodel projections and uncertainties of irrigation water demand under climate change, Geophys. Res. Lett., 40, 4626–4632, https://doi.org/10.1002/grl.50686, 2013.

Wang, H. W., Li, X. B., Wang, D., Zhao, J., He, H. di, and Peng, Z. R.: Regional prediction of ground-level ozone using a hybrid sequence-to-sequence deep learning approach, J. Clean. Prod., 253, 119841, https://doi.org/10.1016/j.jclepro.2019.119841, 2020.

Wilkinson, S. and Davies, W.J., Drought, ozone, ABA and ethylene: new insights from cell to plant to community, Plant Cell Environ., 33, 4, https://doi.org/10.1111/j.1365-3040.2009.02052.x, 2010.

Wu, S., Mickley, L. J., Leibensperger, E. M., Jacob, D. J., Rind, D., and Streets, D. G.: Effects of 2000–2050 global change on ozone air quality in the United States, J. Geophys. Res.-Atmos., 113, D06302, https://doi.org/10.1029/2007JD008917, 2008.

Yadav, D. S., Rai, R., Mishra, A. K., Chaudhary, N., Mukherjee, A., Agrawal, S. B., and Agrawal, M.: ROS production and its detoxification in early and late sown cultivars of wheat under future O_3 concentration, Sci. Total Environ., 659, 200–210, https://doi.org/10.1016/j.scitotenv.2018.12.352, 2019.

Yadav, D. S., Mishra, A. K., Rai, R., Chaudhary, N., Mukherjee, A., Agrawal, S. B., and Agrawal, M.: Responses of an old and a modern Indian wheat cultivar to future O_3 level: Physiological, yield and grain quality parameters, Environ. Pollut., 259, 113939, https://doi.org/10.1016/j.envpol.2020.113939, 2020.

Yadav, D. S., Agrawal, S. B., and Agrawal, M.: Ozone flux-effect relationship for early and late sown Indian wheat cultivars: Growth, biomass, and yield, F. Crop. Res., 263, 108076, https://doi.org/10.1016/j.fcr.2021.108076, 2021.

Yao, A. Y. M.: Agricultural potential estimated from the ratio of actual to potential evapotranspiration, Agr. Meteorol., 13, 405–417, https://doi.org/10.1016/0002-1571(74)90081-8, 1974.

Zanis, P., Akritidis, D., Turnock, S., Naik, V., Szopa, S., Georgoulias, A. K., Bauer, S. E., Deushi, M., Horowitz, L. W., Keeble, J., and Le Sager, P.: Climate change penalty and benefit on surface ozone: a global perspective based on CMIP6 earth system models, Environ. Res. Lett., 17, 024014, https://doi.org/10.1088/1748-9326/ac4a34, 2022.

Zaveri, E. and Lobell, D. B.: The role of irrigation in changing wheat yields and heat sensitivity in India, Nat. Commun., 10, 4144, https://doi.org/10.1038/s41467-019-12183-9, 2019.

Zaveri, E., Grogan, D. S., Fisher-Vanden, K., Frolking, S., Lammers, R. B., Wrenn, D. H., Prusevich, A., and Nicholas, R. E.: Invisible water, visible impact: Groundwater use and Indian agriculture under climate change, Environ. Res. Lett., 11, 084005, https://doi.org/10.1088/1748-9326/11/8/084005, 2016.